

## Histochemical and immunohistochemical changes in rat hepatocytes after halothane exposure

TERUO YAMADA, TAKAKO NOMURA, YUKARI MIKI, SHIGETO KANDA, and JUNZO SASAKI

Department of Cytology and Histology, Okayama University Graduate School of Medicine and Dentistry, 2-5-1 Shikata-cho, Okayama 700-8558, Japan

### Abstract

**Purpose.** Histochemical and immunohistochemical changes were observed in hepatocytes to study the developing and recovery processes of halothane-induced hepatic injury from 0 to 7 days after halothane exposure.

**Methods.** A total of 330 7-week-old male Sprague-Dawley rats, with or without phenobarbital pretreatment, were exposed to halothane in 100%, 21%, 10% oxygen or oxygen alone for 2h.

**Results.** In the phenobarbital group, degenerated hepatocytes were observed immediately after exposure to 10% oxygen, both with and without halothane: glycogen and ribosomal ribonucleic acid (rRNA) disappeared immediately and 6h after exposure, respectively, and necrosis developed in zones 3 to 2 at 6h after exposure. From 12h to day 1, the necrosis was more marked and more widely observed in the cells with halothane than those without halothane. However, all tissues returned to normal by day 7.

**Conclusion.** Disappearance of glycogen at 0h and rRNA at 6h after exposure to halothane under 10% oxygen is considered to be one of the factors inducing necrosis around the central vein. Recovery of the hepatolobular structure was attributed to the rearrangement of the remaining hepatocytes in the portal vein area.

**Key words** Histology · Immunohistology · Halothane · Hypoxia · Hepatic injury

### Introduction

Halothane has been reported to induce hepatic injury [1,2]. This injury has two types: the mild type is seen in 20% of patients (3), and the fulminant type in approximately 1 of 10,000 patients [4]. Although its mechanism remains elusive, some evidence suggests that the protein combines with reactive trifluoroacetyl (TFA), a

halothane metabolite which in vivo induces the immune system to develop hepatitis [5–7]. The reaction of reactive intermediate metabolites (e.g., halothane radical) produced in the process of halothane metabolism with cytochrome P-450 in vivo may be another pathway [8,9]. The occurrence of extreme hypoxia in the hepatocytes due to decrease in hepatic blood flow also causes hepatitis [10].

In the studies on halothane-induced hepatic injury, histological changes in the liver were observed mostly by staining hepatic tissues with hematoxylin–eosin (H-E) and by the development of necrosis in the hepatic central venous area [11,12], which does not permit observation of changes in the intra-hepatocellular substances by H-E staining. One report observed the nutritional state of hepatocytes stained with periodic acid Schiff (PAS) after exposure to halothane [13]. However, intrahepatocellular changes have not been observed histochemically and immunohistochemically.

In the current study, the authors performed histochemical and immunohistochemical studies of intra-hepatocellular changes after halothane exposure using a rat model [14] to evaluate the development and recovery process of halothane-induced hepatic injury, and to contribute to the basic findings in the studies on sevoflurane, isoflurane, enflurane, and desflurane [11,15].

### Materials and methods

All animal experiments were performed according to the guidelines for animal experiments of the Okayama University Medical School.

### Materials

The materials and reagents used in this study were 7-week-old male Sprague–Dawley (SD) rats (Clea Japan,

Osaka, Japan); halothane (Takeda Chemical Industries, Osaka); phenobarbital sodium (Tokyo Chemical Industry, Tokyo, Japan); pentobarbital sodium (Dainippon Pharmaceutical, Osaka); Mayer hemalum solution and Schiff's reagent (PAS) (Merck, Darmstadt, Germany); 4% paraformaldehyde and 1% eosin Y solution (Muto Pure Chemicals, Tokyo); anti-macrophage mouse monoclonal antibody (ED 1) (Serotec, Oxford, England); 5-bromo-2'-deoxyuridine (BrdU), anti-BrdU mouse monoclonal antibody, anti-single-stranded DNA (ssDNA) rabbit polyclonal antibody, anti-mouse or anti-rabbit immunoglobulins conjugated to peroxidase labeled dextran polymer (EnVision+, Peroxidase) and 3,3'-diaminobenzidine (DAB) substrate kit (Dako Japan, Kyoto, Japan); and IATAROZYME TA-Lq (RM163-K) (Iatron Laboratories, Tokyo) as a reagent for analyzing aspartate aminotransferase (AST).

## Methods

### *Animals and procedures*

Male SD rats were divided into two groups: nontreated healthy rats (N group) and rats given water containing 0.1% phenobarbital sodium (PB) ad libitum for 5 days (PB group) before the experiment. The rats of both groups were exposed to 1% halothane (approximately 1 minimum alveolar concentration [MAC]) [16] in 100%, 21%, or 10% oxygen, or 10% oxygen alone without halothane for 2 h. Air was used for 21% oxygen, and air and nitrogen were mixed at the rate of 1 to 1 with an anesthesia apparatus (Model CK-70, Acoma, Tokyo) to make gas containing 10% oxygen. The flow volume of oxygen gas at three different oxygen concentrations was set at 4 l·min<sup>-1</sup> with the anesthesia apparatus. The halothane concentration was adjusted to 1% with a vaporizer (FLUOTEC 3, Cyprane, England). Rats in a polyethylene container (20 × 30 × 10 cm) were exposed to halothane through a tube connected to the halothane vaporizer.

The livers of five rats from each exposure group were collected immediately and at 3 h, 6 h, 12 h, 1 day, 2 days, 3 days, and 7 days after exposure (at 0–12 h, on days 1–7). Five rats each were used under 66 different conditions, i.e., eight different collecting times after 2-h exposures to halothane under three different oxygen conditions or in 10% oxygen alone in two groups, plus the group of rats treated with PB alone, and one control (untreated) group (330 rats in total). The collected livers were studied histochemically and immunohistochemically for general cell structure, glycogen in the cells, apoptosis, ribosomal ribonucleic acid (rRNA) granules, cell infiltration, and proliferation of hepatocytes. When the liver was collected, 3 ml of the blood was collected

in a heparinized glass syringe from the left ventricle to determine the AST concentration in the blood with the reagent (IATAROZYME TA-Lq kit). The five specimens taken under each test condition were used to determine the AST values.

### *Morphological and immunohistochemical studies*

The liver was excised after perfusion through the portal vein (PV) with 4% paraformaldehyde (4% PFA), cut into pieces 2–3 mm thick, and fixed in 4% ice-cooled PFA. The sections were dehydrated according to routine procedures, embedded in paraffin, and cut into pieces in 5 μm thick and stained with H-E, PAS, and methylgreen pyronin (MGP).

Arbitrarily selected paraffin-removed sections were immersed in 3% H<sub>2</sub>O<sub>2</sub>/MtOH at room temperature for 10 min to dispose the intrinsic peroxidase, and immersed in trypsin solution (1 mg trypsin·ml<sup>-1</sup> 0.1 M PBS) at 37°C for 30 min to identify the infiltrated and apoptotic cells. Then, ED 1 and anti ssDNA antibodies (rabbit) were used as the primary antibodies to identify infiltrated and apoptotic cells, respectively. EnVision+ and peroxidase (mouse or rabbit) were used as the secondary antibodies to make the target cells emit colors with a DAB substrate kit.

To study hepatocellular proliferation, BrdU 50 mg·kg<sup>-1</sup> dissolved in 1 ml of PBS was administered intraperitoneally 2 h before liver resection. The rats underwent median abdominal incision under pentobarbital anesthesia. Then, the liver was excised, immersed in 70% ice-cooled ethanol, dehydrated, and embedded in paraffin. After the liver was cut into 5-μm sections, the slide glasses were immersed in 3% H<sub>2</sub>O<sub>2</sub>/MtOH. Anti BrdU mouse monoclonal antibody was used for the primary antibody, and EnVision+ and peroxidase (mouse) were used for the secondary antibodies.

### *Numerical analysis of serum AST values and the area negatively stained with PAS after halothane exposure*

From 0 h to 7 days after exposure to halothane, AST values in the serum collected from five rats were analyzed by the statistical tests mentioned below to compare them with values of the control group and to compare values collected at different times.

First, as the interaction was found between halothane exposure and time, the data were analyzed by one-way analysis of variance (ANOVA). There was a significant difference in the values according to ANOVA ( $P < 0.001$ ). The data were further analyzed by an equal variance test, and the analyzed data showed various distributions by this test. Then the data were analyzed again by a Kruskal-Wallis test to get a significant difference ( $P < 0.001$ ). Last, each value thus obtained was

compared by a multiple-comparison test. The value of  $P < 0.01$  was assumed significant.

The area of the lobule negatively stained with PAS was expressed as a percentage of the liver lobule. The length of the lobule from the central vein (CV) to the portal vein (PV) was measured as  $a$ , and the length of the PAS-negative area from the CV to PV as  $b$ , to calculate the PAS-negative area as a percentage of the lobule ( $y$ ) as follows:  $y(\%) = b/a \times 100$ . Straight lines of the sinusoid running from the PV to the CV were selected to measure the length of  $a$  and  $b$ .

At each collecting time,  $a$  and  $b$  were measured in the 25 samples that had been taken from five different regions in the lobules of five rats. The mean percentage of the PAS-negative area ( $Y$ ) was obtained from these 25 ( $y$ ) samples ( $Y$ : mean  $\pm$  SD). Each value of  $Y$  was analyzed by the same statistical tests as mentioned above, to compare them with values of the control group and to compare values from different collecting times.

## Results

### Time course changes in serum AST after exposure

The AST values (mean  $\pm$  SD) of rats in the control and PB-pretreated alone groups were  $48.6 \pm 4.0$  and  $51.4 \pm 5.5$  U, respectively. The AST values in both the PB and the N groups after halothane exposure under 100% and 21% oxygen, or exposure to 10% oxygen alone, differed little from those of the control group (Fig. 1).

The AST values differed from those of the control group in the PB group after halothane exposure under 10% oxygen. The AST values were significantly higher than those of the control group ( $P < 0.01$ ) from 6 h to day 2, reached the peak level ( $222.2 \pm 18.9$  U) on day 1, and then returned to the normal level on day 7. In the N group, the AST values were slightly higher than those of the control group from hour 3 to day 1, reached the peak level ( $83.0 \pm 12.5$  U) at hour 12, and then returned to the normal level on day 2. The AST values at hour 12 on days 1 and 2 were significantly different ( $P < 0.01$ ).

### Histochemical changes

The images of the liver tissues in control rats are shown in Figs. 2a, 3a, and 4a. The images of rats pretreated with PB alone appeared to be almost the same as those of control rats.

In the N group, no histochemical changes were seen in cells exposed to halothane for 2 h under 100% or 21% oxygen compared with control images. However, after 2 h of halothane exposure under 10% oxygen, PAS staining decreased to approximately  $38.2 \pm 4.6\%$  (zone

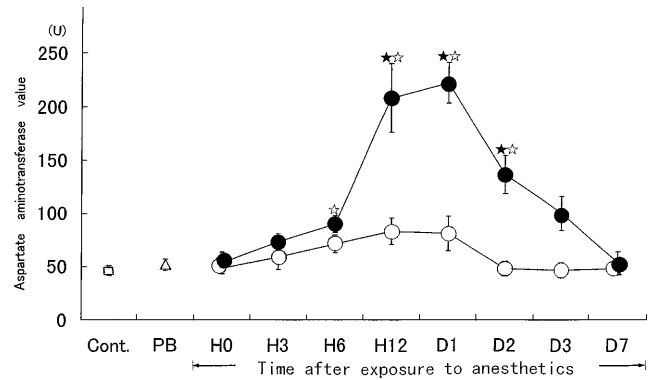


**Fig. 1.** Changes in serum aspartate aminotransferase (AST) values (mean  $\pm$  SD) of control rats, rats pretreated with phenobarbital (PB) alone, and rats exposed to halothane under 10% oxygen during the period from hour 0 to day 7 in the group pretreated with PB and the normal (N) group not pretreated with PB. (□) AST values of the control ( $48.6 \pm 4.0$  U); (Δ) AST values of the PB group before exposure ( $51.4 \pm 5.5$  U); (○) AST values of the N group exposed to halothane in 10% oxygen; (●) AST values of rats in the PB group exposed to halothane in 10% oxygen; (☆) significantly different from the control group ( $P < 0.01$ ); (★) significantly different at each collecting time (at hour 0–hour 12, on days 1–7) between PB and N groups ( $P < 0.01$ ). Not different between PB and N groups, data from rats exposed to 100% and 21% oxygen were omitted. (H) Hour; (D) day

2) at hour 0,  $25.0 \pm 3.7\%$  at hour 3, and  $10.1 \pm 3.3\%$  (zone 3) at hour 6 from the CV to the PV, and returned to the level of the control group at hour 12 (Fig. 5).

In the PB group, there were no changes in PAS staining under 100% oxygen as compared with the control group. However, PAS staining decreased after 2 h of halothane exposure under 21% oxygen and recovered in the same manner as in the N group. Marked changes were observed in the cells when exposed to halothane for 2 h under 10% oxygen. By PAS staining, approximately  $56.3 \pm 7.0\%$  of the area (zones 3 to 2) from the CV to the PV was PAS-negative from hour 0 to day 1. The PAS-negative area decreased from day 2 to day 3 and returned to normal by day 7 (Figs. 2 and 5). By MGP staining, rRNA granules disappeared in one or two layers in the PAS-negative cells around the CV at hour 0. From hour 3 to day 3, rRNA granules completely disappeared in the PAS-negative cells (Fig. 3). By H-E staining, the cells in the PAS-negative area were homogeneously stained with eosin. From hour 12 to day 1, large vacuoles formed in the boundary between the part of the PAS-negative area in the CV and the part of the PAS-positive area in the PV. These large vacuoles were not visible on day 2 (Fig. 4).

In the N group, no changes were seen in the liver tissues in 10% oxygen alone for 2 h. In the PB group, however, PAS-negative cells appeared in zone 3 at hour 0 after 2 h exposure to 10% oxygen alone. In this PAS-

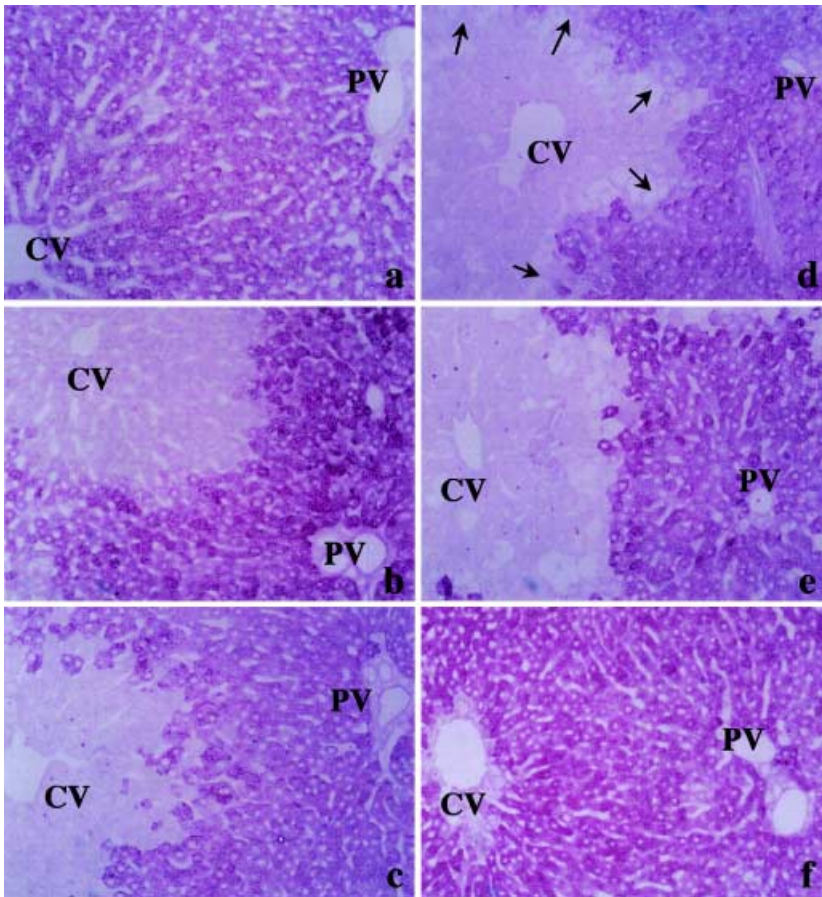


**Fig. 2.** Changes in hepatocytes stained with periodic acid Schiff (PAS) after halothane exposure under 10% oxygen in the PB group. **a** In this image from the control group, PAS-positive reaction is evenly distributed from the portal vein (PV) to the central vein (CV) ( $\times 480$ ). **b** At hour 0, the PAS-negative area is observed in zones 3 to 2 ( $\times 480$ ). **c** At hour 6, the PAS-negative area is almost identical to the image at hour 0, but in this area cell swelling and fusion have begun to appear ( $\times 480$ ). **d** At hour 12, the PAS-negative area is almost identical to the image at hour 6, but large vacuoles shown with *arrows* have appeared in the boundary between the PAS-negative area around the CV and the PAS-positive area around the PV ( $\times 480$ ). **e** On day 1, the image is almost identical to that at hour 12. ( $\times 480$ ). **f** On day 3, the PAS-negative area is much smaller than on day 1 ( $\times 480$ ).

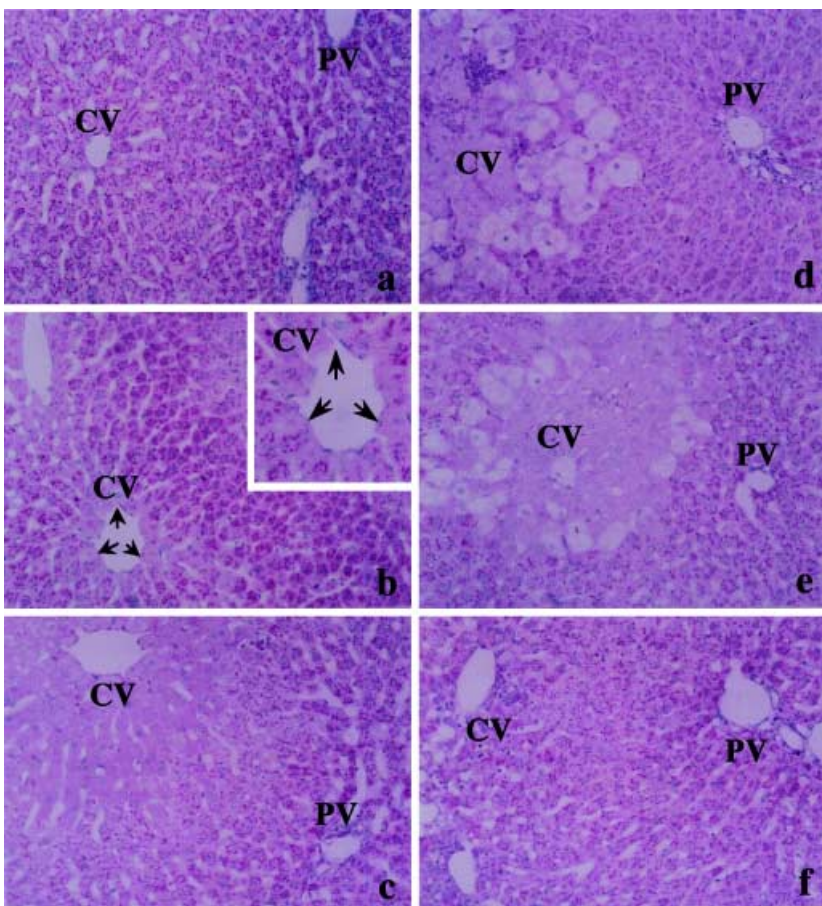


**Fig. 3.** Changes in hepatocytes stained with methylgreen pyronin (MGP) after halothane exposure under 10% oxygen in the PB group. **a** In this image from the control group, rRNA granules positively stained with MGP are evenly distributed from the PV to the CV ( $\times 480$ ). **b** At hour 0, rRNA has begun to disappear in one or two layers of the cells around the CV. The *arrows* indicate the cells where rRNA disappeared ( $\times 480$ ). The *upper right* photo is the magnified part of the CV ( $\times 800$ ). **c** At hour 6, rRNA completely disappeared in the PAS-negative area ( $\times 480$ ). **d** At hour 12, the image is almost identical to that at hour 6, and large vacuoles are observed in the boundary between PAS-negative and -positive areas ( $\times 480$ ). **e** On day 1, the image is almost identical to that at hour 12 ( $\times 480$ ). **f** On day 3, rRNA disappearance in the PAS-negative cells is observed in three to four layers of cells around the CV ( $\times 480$ ).

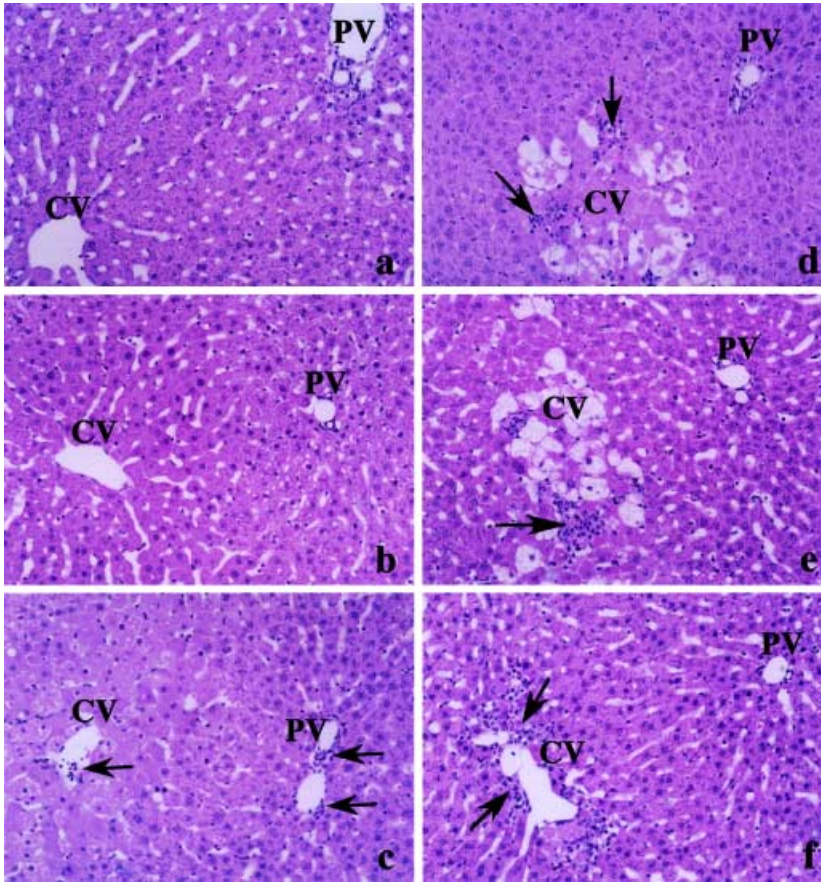


**Fig. 4.** Changes in hepatocytes stained with hematoxylin-eosin (HE) after halothane exposure under 10% oxygen in the PB-group. **a** The image of the control ( $\times 480$ ). **b** At hour 0, the image of the exposed liver section is almost identical to that of the control ( $\times 480$ ). **c** At hour 6, cells in the PAS-negative area are swollen, and vacuoles, pyknosis, and cell fusion have appeared. The cells are homogeneously stained with eosin. The infiltrated cells shown with *arrows* have begun to disperse in the PAS-negative area ( $\times 480$ ). **d** At hour 12, cells in the PAS-negative area are swollen, and pyknosis, cell fusion, and denudation are visible. Large vacuoles have appeared in the boundary between PAS-negative and -positive areas. Many infiltrated cells are visible in the PAS-negative area (*arrows*) ( $\times 480$ ). **e** On day 1, the image is almost identical to that at hour 12 ( $\times 480$ ). **f** On day 3, cells in the PAS-negative area are fused, although vacuoles have disappeared, and the cells are homogeneously stained with eosin. Numerous infiltrated cells are observed around the CV (*arrows*) ( $\times 480$ )

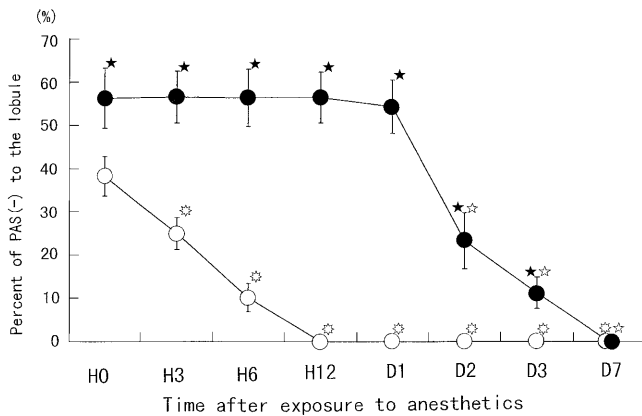


**Fig. 5.** Numerical analysis of changes in the PAS-negative area in the liver at each collecting time after halothane exposure. Each collecting time value was calculated as described in the Methods. (●) PB group. Unchanged until day 1, when Y values ( $56.3 \pm 7.0\%$  at hour 0) began to decrease from day 2 until they disappeared on day 7. (○) N group. Y values ( $38.2 \pm 4.0\%$  at hour 0) disappeared at hour 12. (☆) (PB-group): significantly different compared with those from hour 0 to day 1 ( $P < 0.01$ ). (⊛) (N-group): significantly different compared with that at hour 0 ( $P < 0.01$ ). (★) Significantly different at each collecting time (at hour 0–hour 12, on days 1–7) between PB and N groups ( $P < 0.01$ ). (H) Hour; (D) day

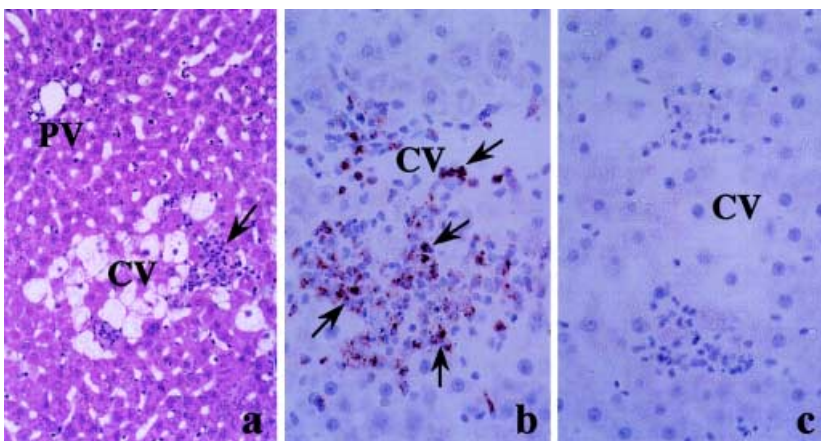


**Fig. 6.** Images of infiltrated cells in the PB group at hour 12 after 2h of halothane exposure under 10% oxygen. **a** The image of the infiltrated cells (*arrows*) stained with HE at hour 12 after halothane exposure ( $\times 520$ ). **b** The image of the infiltrated cells (*arrows*) reacting to antimacrophage mouse monoclonal antibody (ED 1) ( $\times 870$ ). **c** The image of the negative control of **b** ( $\times 870$ )

negative area, the cells were slightly swollen, rRNA granules appeared in the cells at hour 6, and vacuolated cells appeared at hour 12, while rRNA granules had completely disappeared, but the tissue recovered to the normal hepatolobular structure on day 2.

#### *Immunohistochemical observation*

Infiltrated cells began to appear from hour 3 in the PAS-negative area in the PB group. Many infiltrated cells in the PAS-negative area cross-reacted with ED 1, which indicated that they were macrophages (Fig. 6). The reaction of the BrdU intake or ssDNA was not observed until day 7, which showed that neither hepatocellular proliferation nor apoptosis appeared after halothane exposure.

#### *PAS-negative area of the hepatic lobule after exposure*

Figure 5 shows changes over time in the PAS-negative area after halothane exposure under 10% oxygen in the PB and N groups.

In the PB group, the mean percentage of the area of the lobule that was PAS-negative was approximately  $56.3 \pm 7.0\%$  (zones 3 to 2) from hour 0 until day 1, decreased to approximately  $23.3 \pm 6.5\%$  on day 2 ( $P < 0.01$ ), and became zero on day 7. The differences between 0 and day 1 and between day 2 and day 3 were significant ( $P < 0.01$ ).

In the N group, the PAS-negative area was significantly smaller at hour 0 than at hour 3 and hour 6 ( $P < 0.01$ ). In the PB group, the PAS-negative area was approximately 1.5 times larger than that of the N group at hour 0 ( $P < 0.01$ ). Significant differences were found at each collecting time between the PB and the N groups from hour 0 to day 3 ( $P < 0.01$ ).

## **Discussion**

Glycogen (at hour 0) and rRNA (at hour 6) disappeared in the early stage from the hepatocytes in zones 3 to 2 of the liver after halothane exposure under 10% oxygen. This is a new finding in the study of halothane-induced hepatic injury.

In many studies on halothane-induced hepatic injury, necrosis has been observed around the CV [11,12], but its etiology has not been clarified yet [17–20].

One percent halothane (approximately 1 MAC) [16] was used. A 2-h exposure was adopted, because more than 1.5h was needed to obtain a constant halothane concentration in the blood according to the report by Nishizaki [21].

MacDonald et al. [22] reported that liver dysfunction may be caused by hypoxia per se if the level of hypoxia

is severe and if the inspired oxygen tension is less than 10%. The changes in serum AST levels and the necrosis in the CV until day 1 in the current study were consistent with the reports by Ross et al. [23] and Knights et al. [13].

The disappearance of rRNA granules in the PAS-negative area after halothane exposure under 10% oxygen may be attributed to the inhibition of synthesis from DNA to rRNA, although it is not clear yet whether the synthesis is inhibited by halothane itself, anoxia, or reductive halothane metabolites. The cells in the PAS-negative area may have exhausted substances necessary for energy transfer after halothane exposure, and transcription from DNA to rRNA has been inhibited to prevent various protein syntheses. In a previous study by the authors [24], cytochrome P-450 decomposed and free heme with cytotoxicity increased causing hepatocellular injury after halothane exposure under hypoxia for 2h. Cellular injury with decomposition of cytochrome P-450 by halothane exposure is attributed to the lack of heme oxygenase-1 synthesis and cytotoxic heme in the cells when intracellular energy is lost and rRNA disappears, as seen in the current study.

Rorie et al. [25] and Rose et al. [26] reported that epinephrine and norepinephrine were neuronally released by halothane exposure under hypoxia, causing hepatic vascular contraction. Cooperman [27], Frink et al. [28], and Nishizaki [21] reported that hepatic arterial vascular resistance (HAVR) increased during and after halothane exposure in dogs. In the current study, it appears that hepatic vascular contraction occurred, HAVR increased during halothane exposure under 10% oxygen, and severe hypoxia in the liver continued until day 1. If this interpretation is correct, the cells suffered from severe hypoxia from hour 0 to day 1, causing a decrease in the oxygen supply/demand ratio in the area from zones 3 to 2, and the cells around the CV had exhausted glycogen immediately after halothane exposure. Necrotic degeneration followed in a wide area. From day 2, the necrotic area began to shrink.

Although Ross et al. [23] and Knights et al. [13] reported that mitosis occurred in the liver at hour 48, in this study BrdU intake was not observed until day 7, which showed no hepatocellular regeneration after the exposure. Knights et al. [13] observed mitosis, but they used a milder oxygen condition (14% oxygen concentration) for halothane exposure than we did (10% oxygen concentration, with and without halothane). Apoptosis was not observed from hour 0 to day 7, when we stained liver sections using anti-ssDNA rabbit polyclonal antibody. According to Kerr et al. [29], necrosis occurred when hypoxia was severe, whereas apoptosis occurred when hypoxia was mild, which might explain why we could not find apoptosis under 10% oxygen. As Rozga et al. [30] described, halothane-

related necrosis may recover due to the compression of necrotic cells by densely packed hepatocytes after the hepatocytes migrate from the periphery to the necrotic area in the central lobule, eventually occluding the interposed sinusoidal lumen. In the current study also, the hepatolobular structure is considered to have recovered due to the rearrangement of the remaining hepatocytes in the PV area along the hepatic cell cords.

In conclusion, glycogen at hour 0 and rRNA at hour 6 disappeared from zones 3 to 2 after halothane exposure under 10% oxygen among rats in the PB group. Glycogen and rRNA disappeared in the hepatocytes, causing inhibition of rRNA synthesis and development of necrosis in the hepatocytes around the CV. In the necrotic area, macrophages appeared from hour 12 to day 2, but neither apoptosis nor proliferation was observed in hepatocytes after halothane exposure.

*Acknowledgments.* We wish to thank Dr. Akihiko Seki, Department of Public Health, Graduate School of Medicine and Dentistry, Okayama University, for his helpful advice for our statistical analyses.

This work was supported in part by a Grant-in-Aid for Scientific Research (C) (1998–1999, No.10671415) from the Ministry of Education, Science, Sports and Culture, Japan.

## References

- Virture RW, Payne KW (1958) Postoperative death after flouthane. *Anesthesiology* 19:562–563
- Brody GL, Sweet RB (1963) Halothane anesthesia as a possible cause of massive hepatic necrosis. *Anesthesiology* 24:29–37
- Wright R, Eade OE, Chisholm M, Hawksley M, Lloyd B, Moles TM, Edwards JC, Gardner MJ (1975) Controlled prospective study of the effect on liver function of multiple exposures to halothane. *Lancet* 1:817–820
- Moult PJA, Sherlock S (1975) Halothane-related hepatitis. A clinical study of twenty-six cases. *Q J Med* 173:99–114
- Neuberger J, Mieli-Vergani G, Tredger JM, Davis M, Williams R (1981) Oxidative metabolism of halothane in the production of altered hepatocyte membrane antigens in acute halothane-induced hepatic necrosis. *Gut* 22:669–672
- Kenna JG, Satoh H, Christ DD, Pohl LR (1988) Metabolic basis for a drug hypersensitivity: antibodies in sera from patients with halothane hepatitis recognize liver neoantigens that contain the trifluoroacetyl group derived from halothane. *J Pharmacol Exp Ther* 245:1103–1109
- Njoku D, Laster MJ, Gong DH, Eger EI II, Martin JL (1997) Biotransformation of halothane, enflurane, isoflurane, and desflurane to trifluoroacetylated liver proteins: association between protein acylation and hepatic injury. *Anesth Analg* 84:173–178
- Massion WH, Poyer JL, Downs P, Fagraeus L (1984) Comparative study of halogenated hydrocarbon toxicity and free radical formation in rat liver. *Anesthesiology* 61:A-274
- Rosenberg PH, Wahlstrom T (1973) Trifluoroacetic acid and some possible intermediate metabolites of halothane as haptens. *Anesthesiology* 38:224–227
- Shingu K, Eger EI II, Johnson BH (1982) Hypoxia may be more important than reductive metabolism in halothane-induced hepatic injury. *Anesth Analg* 61:824–827
- Van Dyke RA (1982) Hepatic centrilobular necrosis in rats after exposure to halothane, enflurane, or isoflurane. *Anesth Analg* 61:812–819
- Gelman S, Van Dyke RA (1988) Mechanism of halothane-induced hepatotoxicity: Another step on a long path. *Anesthesiology* 68:479–482
- Knights KM, Gourlay GK, Hall P de la M, Adams JF, Cousins MJ (1987) Halothane hepatitis in an animal model: time course of hepatic damage. *Br J Exp Path* 68:613–624
- McLain GE, Sipes IG, Brown BR (1979) An animal model of halothane hepatotoxicity: Roles of enzyme induction and hypoxia. *Anesthesiology* 51:321–326
- Strum DP, Eger EI II, Johnson BH, Steffey EP, Ferrell LD (1987) Toxicity of sevoflurane in rats. *Anesth Analg* 66:769–773
- Quasha AL, Eger EI II, Tinker JH (1980) Determination and applications of MAC. *Anesthesiology* 53:315–334
- Cohen EN, Trudell JR, Edmunds HN, Watson E (1975) Urinary metabolites of halothane in man. *Anesthesiology* 43:392–401
- Brown BR Jr, Sipes IG, Baker RK (1977) Halothane hepatotoxicity and the reduced derivative, 1,1,1-trifluoro-2-chloroethane. *Env Health Perspect* 21:185–188
- Schieble TM, Costa AK, Heffel DF, Trudell JR (1988) Comparative toxicity of halothane, isoflurane, hypoxia, and phenobarbital induction in monolayer cultures. *Anesthesiology* 68:485–494
- Johnson ME, Sill JC, Uhl CB, Van Dyke RA (1993) Effect of halothane on hypoxic toxicity and glutathione status in cultured rat hepatocytes. *Anesthesiology* 79:1061–1071
- Nishizaki S (1987) Effect of halothane anesthesia on systemic and hepatic circulation in dog. *Okayama Igakkai Zasshi* 99:643–655 (in Japanese, with English abstract)
- MacDonald AC, Marble AE, Perkins JG (1979) Hepatic blood flow and metabolism. *Arch Surg* 114:616–622
- Ross WT, Daggy BP, Cardell RR (1979) Hepatic necrosis caused by halothane and hypoxia in phenobarbital-treated rats. *Anesthesiology* 51:327–333
- Odaka Y, Takahashi T, Yamasaki A, Suzuki T, Fujiwara T, Yamada T, Hirakawa M, Fujita H, Ohmori E, Akagi R (2000) Prevention of halothane-induced hepatotoxicity by hemin pretreatment: protective role of heme oxygenase-1 induction. *Biochem Pharmacol* 59:871–880
- Rorie DK, Tyce GM (1983) Effects of hypoxia on norepinephrine release and metabolism in dog pulmonary artery. *J Appl Physiol* 55:750–758
- Rose CE JR, Althaus JA, Kaiser DL, Miller ED, Carey RM (1983) Acute hypoxemia and hypercapnia: increase in plasma catecholamines in conscious dogs. *Am J Physiol* 245:H924–H929
- Cooperman LH (1972) Effects of anaesthetics on the splanchnic circulation. *Br J Anaesth* 44:967–970
- Frink EJ Jr, Morgan SE, Coetzee A, Conzen PF, Brown BR Jr (1992) The effects of sevoflurane, halothane, enflurane, and isoflurane on hepatic blood flow and oxygenation in chronically instrumented greyhound dogs. *Anesthesiology* 76:85–90
- Kerr JFR (1971) Shrinkage necrosis: a distinct mode of cellular death. *L Pathol* 105:13–20
- Rozga J, Jeppsson B, Bengmark S (1986) Portal branch ligation in the rat. Reevaluation of a model. *Am J Pathol* 125:300–308